Surface & Coatings Technology 228 (2013) S150–S154

Contents lists available at SciVerse ScienceDirect

Surface & Coatings Technology

journal homepage: www.elsevier.com/locate/surfcoat

The characteristics of $Cd_xSn_{1-x}O$ films prepared by RF magnetron sputtering from powder targets

Y.W. Zhou *, X. Liu, F.Y. Wu, C.K. Zhang, X.Y. Zhang

School of Materials and Metallurgy, University of Science and Technology Liaoning, No.185 Qianshan Rd., Hi-tech District, Anshan, Liaoning 114051, China

ARTICLE INFO

Available online 4 July 2012

Keywords:
Multi-component TCO film
Powder targets
RF sputtering
Closed-field unbalanced magnetron sputtering

ABSTRACT

Transparent conductive cadmium and tin oxide films ($Cd_xSn_{1-x}O$ TCO) prepared by RF magnetron sputtering from the mixed oxide powder targets were with similar compositions to those of the targets. The morphological structures of the films were columnar in the grain sizes over 100 nm. New phrases were formed for the films with proper metallic ratio, i.e. x = 0.5 and 0.7 and the mixture of nano-crystal and amorphous structure might exist. Also, the nano-crystal structure with severe lattice deformation could be seen in the x = 0.2 and 0.8 films, and all nano-crystals were in domain sizes about 10–20 nm. Other multi-component films were with amorphous structure. The average transmittance of the films within the visible wavelength, except for the pure CdO film, was over 80%. The concentrations of electrons of these n-type $Cd_xSn_{1-x}O$ films were in the order of 10^{20} cm^{-3}. Without considering of the pure CdO and SnO_2 films, the high mobilities (up to 50 $cm^2/V\,s$) can be obtained from the films with amorphous structure. The resistivities of the films decreased from 10^{-3} to $10^{-4}\,\Omega\cdot cm$ with the increases of Cd ratios in the films.

1. Introduction

It is well known that transparent conductive oxide (TCO) films can be widely used as the passive layer, such as the electrode and window layer in photovoltaic solar cell [1–5]. Tin doped indium oxide (ITO), aluminum doped zinc oxide (AZO) and fluorine doped tin oxide (FTO) are quite commonly used n-type materials for above application [1,6–9]. With the development of multi-component TCO materials, these films obtained the chances to be used as an active layer, such as in thin film transistor, due to the amorphous structure and therefore, the high carrier mobilities since 2006 [10,11], in which the channel mobility of 12–20 $cm^2/V\,s$ could be achieved. The recent studies on multi-component TCO materials varied from the selection of the oxides (indium, zinc, gallium, tin (SnO_2), strontium and Hafnium) [12–15] focused on not only the as-prepared and post treatment processes, such as magnetron sputtering, pulsed laser deposition and solution-process, annealing atmosphere and temperature, but also the substrate, compositions and carrier's density and mobility [13,16–23]. All the research studies aimed to produce the TFT with high mobility and stability at low temperature. Apart from the amorphous multi-component oxide TFT, Fortunato E et al. [1] reported the fully transparent TFT by using undoped ZnO as the channel layer.

Another important oxide material, cadmium oxide (CdO), which was the first known TCO material and famous for the very high carrier's mobility and low resistivity [24–26], but notorious for the low transmittance and narrow band gap [24,27] should not be forgotten. Several multi-component CdXO films, deposited by sol–gel, MOCVD and magnetron sputtering etc., were studied to adjust the band gaps and transmittance of the films, in which X could be In, Zn, Ga, Sn, carbon (C) and silicon (Si) [28–33].

CdO and SnO_2 were selected in this study by changing the oxide proportions to form the $Cd_xSn_{1-x}O$ films either with crystal or amorphous structure, high transmittance, various band gaps, low resistivity and high carrier's mobility. Closed-field unbalanced magnetron sputtering from powder targets by pulsed DC has been successfully used over recent years taking its advantages of cheap target fabrication and easy changes of the target compositions [7,8]. Instead of Pulsed DC, a RF 600X drive, which produced even high plasma density and low ion energy, was used in this study [34,35]. The aim of the investigation is to figure out the effect of the Cd:Sn ratio on the structure, the optical and electrical properties of the $Cd_xSn_{1-x}O$ films. Also, it will be helpful to find out the relationship between the structures and properties of the ternary films. There must be potential to produce $Cd_xSn_{1-x}O$ films with desirable features according to the application requirements by adjusting the compositions and controlling the process parameters.

2. Experimental details

The $Cd_xSn_{1-x}O$ coatings were deposited in a rig specifically designed for the use of powder targets [7,35,36]. The substrate holder was positioned directly above the magnetron, at a separation of 150 mm. The target was connected with a RF drive.

* Corresponding author. Tel.: +86 412 5929360; fax: +86 412 5929525.
E-mail address: zhouyanwen@yahoo.com (Y.W. Zhou).

0257-8972/$ – see front matter © 2012 Elsevier B.V. All rights reserved.
doi:10.1016/j.surfcoat.2012.06.079

The 99.99% pure CdO and SnO_2 powders, micrometers in size, were mixed as appropriate atomic ratios, and blended in a rotable drum for several hours to get the uniform compositions. The particles of the powders can be seen from the SEM photography in Fig. 1 and the composition of the powder targets referred in Table 1. The mixed powder was distributed across the surface of a copper backing plate on the magnetron, slightly tamped down using a cylindrical stainless steel block, to produce a 2 mm uniform thickness and smooth surface to the targets. No further process, such as sintering, was involved in the target production. The rig was then evacuated to a base pressure of lower than 2×10^{-3} Pa and backfilled with Argon gas to a pressure of 0.2 Pa. The glass microscope slides (soda-lime silicate of 25.4×76.2 mm^2 in dimension) as the substrates were ultrasonically cleaned in ethanol, and then inner plasma cleaned in the chamber by RF at 100 W for 15 min. The substrates were then deposited at 200 W RF power for 3 h to obtain sufficient coating's thicknesses for the analysis of the XRD structures and electrical properties. Three slides were deposited in one run to make sure there would be enough samples to be analyzed and compared. Before inner cleaning, each glass slide was drawn an ink line. The coated ink line was able to be removed by ethanol after deposition and left a step on the coating. These coating steps can be used to measure the thicknesses of the films.

The AZO and multi-component ITO and AZO films were deposited by pulsed magnetron sputtering from AZO (3% Al) and ITO + AZO mixed powder targets in our previous study [37]. The compositions of the films across the sections (or through the thickness) were analyzed by secondary ion mass spectroscopy (SIMS) and Rutherford backscattering (RBS) techniques, which proved the uniform, similar compositions to those of the targets. The possible reason might be that the atoms on the surface of the powder target got the same chance to be sputtered out, no matter how different the sputtering rates of the oxides are. Anyway, two samples were taken in this study for the examinations by X-ray photoelectron spectroscopy (XPS) and energy dispersive spectrum analysis (EDS), to get the surface compositions of the films. The structures of the coatings were subsequently characterized by atomic force microscopy (AFM) and transmission electron microscopy (TEM) to show the morphological structure and micro-structure, and by X-ray diffraction (XRD) to determine the preferred orientations. The coatings were scratched off from the glass slide substrates, and then put into ethanol, finally fished out by micro-grid wires to be ready as the TEM samples. Coating thicknesses were measured across the film steps by an Afar surface profilometer. The electrical properties were investigated using Hall-effect (HMS-3000). Optical transmittance of the films was taken within the ultraviolet, visible and near-infrared wavelength (200–1100 nm) by a spectrophotometer (UV-2802S). The transmittance of the actual film was defined as the measured transmittance after deducting the glass background.

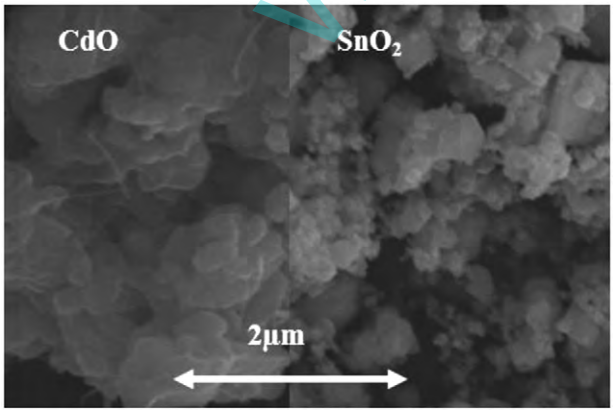

Fig. 1. SEM photography of the oxide powder.

3. Results and discussion

3.1. Composition and structure

From the earlier study [37], it can be presumed that the composition of the film through thickness should be uniform and the same as those of the targets due to the equal chances of the oxide atoms to be sputtered out from the surface of the target. To confirm the above assumption, two samples were measured by using of XPS and EDS techniques. The measured and fitted XPS spectra can be seen in Fig. 2. The atomic ratios of Cd:Sn were calculated after fitting, and the results were compared to those of the EDS measurement, see Table 1. The measured and calculated Cd:Sn ratios were close to those of the targets. Therefore, we may conclude that the compositions of the targets should be able to represent those of the films.

AFM analysis showed that the films were columnar in the grain sizes over 100 nm, refer to Fig. 3. There was no evidence relating columnar grain sizes to the compositions of the $Cd_xSn_{1-x}O$ films. The surface roughnesses of the films were directly analyzed by using the CSPM imaginer software, which was provided by the AFM sale represent. The surface roughnesses of the ternary component films became much lower than those of the pure oxide films. The average roughnesses of the pure CdO and SnO_2 films were 21.6 nm and 2.2 nm, respectively. The average roughnesses of the multi-component films were less than 1 nm. The $Cd_xSn_{1-x}O$ films ($x=0.4$–0.7) were either the mixture of nano-crystal and amorphous structures or amorphous structure, refer to the TEM micrograph in Fig. 4. The structure of the other films was nano-crystalline. The domain sizes of the nano-crystals were about 10–20 nm. The differences of the roughness of the pure oxide films may be due to the big differences of the deposition rates. Therefore, the columnar grains of CdO film grew much faster than those of the SnO_2 film. The very smooth roughness of the ternary oxide films may benefit from the amorphous structure [13,38].

The (111) and (200) preferred orientations of pure CdO and (200) of pure SnO_2 films were shown in the XRD patterns, refer to Fig. 5. (200) CdO orientation could be seen for the film with $Cd_{0.8}Sn_{0.2}O$ due to the Sn atom doping into CdO. The position of CdO (200) was very near to SnO_2 (200) in the XRD spectra, and with similar lattice distances. Hence, tin atoms would be easy to place themselves onto the positions of cadmium atoms with the CdO orientation (200). There was no diffraction peak in the $Cd_{0.2}Sn_{0.8}O$ film, which was supposed to be SnO_2 (200). The reason might be the severe lattice deformation, small nano-crystal sizes and the relatively thin thickness (408 nm) of the film. Also, it was possible that the broad peaks in the $Cd_{0.7}Sn_{0.3}O$ and $Cd_{0.5}Sn_{0.5}O$ XRD spectra were the new Cd_2SnO_4 and $CdSnO_3$ phrases with the preferred orientations of (200) and (020), respectively [24]. The new phrases were considered due to the proper compositions of the coatings. The diffraction peaks of the new phrases were with wide 'full width at half maximum' (FWHM), which meant that the crystal sizes were even smaller than those of the pure oxide films, or the deformation of the new phrases' lattice was serious and more or less amorphous structure might exist. Others showed no obvious orientations, which might be due to the amorphous structure in the films. The metallic atoms tend to position themselves randomly and only connect with the oxygen atoms when the proportions of the metallic atoms are similar to each other. Therefore, the short range order of atoms, which is the special feature of the amorphous structure, might be formed.

3.2. Optical properties

The average transmittance of the $Cd_xSn_{1-x}O$ films within the visible wavelength was about 80%, except for that of the pure CdO film (60%), see Fig. 6. The tangent lines were drawn at the beginnings of the α^2~hω curves, which were transferred from the transmittance

Table 1
Thickness and composition and electrical properties of $Cd_xSn_{1-x}O$ films.

Compositions of targets	EDS measurement	XPS calculation	Film thickness (nm)	Concentration $\times 10^{20}$ (cm^{-3})	Mobility cm^2/V s	Resistivity $\times 10^{-3}$ ($\Omega \cdot cm$)
SnO_2	N/A	N/A	355	−0.319	5.55	35.6
Cd:Sn = 1:4	N/A	N/A	408	−1.518	15.5	2.66
Cd:Sn = 2:3	2:3.26	2:2.86	522.9	−1.382	43.4	1.04
Cd:Sn = 1:1	N/A	N/A	683.3	−2.200	32.35	0.877
Cd:Sn = 3:2	N/A	N/A	716.7	−2.060	50.4	0.602
Cd:Sn = 7:3	N/A	N/A	604.8	−3.158	43.14	0.458
Cd:Sn = 4:1	4:1.07	4:1.04	1513.9	−5.618	25.5	0.436
CdO	N/A	N/A	1569	−1.59	57.7	0.682

spectra, Fig. 7. The absorption coefficient (α) was calculated according to the equation

$$\alpha = \left(\frac{1}{t}\right) \ln\left(\frac{1}{T}\right) \quad (1)$$

where t is the film's thickness, and T is the transmission at the wavelength in question [30]. The calculation in reference [30] showed that the reflectance of the film only contributes 0.05 eV band gap difference, and therefore, was reasonable to calculate 'α' by Eq. (1). Then the intercepts of the tangent lines on the hω axis could be defined as the band gaps of the films. It could be clearly seen from the inner drawing of Fig. 7 that the band gaps of the $Cd_xSn_{1-x}O$ films were between those of pure CdO and SnO_2 films, and directly related to the metallic components of the films. The decreases of Sn and increases of Cd in the films would lead to the reductions of the band-gaps. The band gaps can be adjusted by varying the metallic components of the $Cd_xSn_{1-x}O$ films and the transmittance can be improved by adding SnO_2 into CdO.

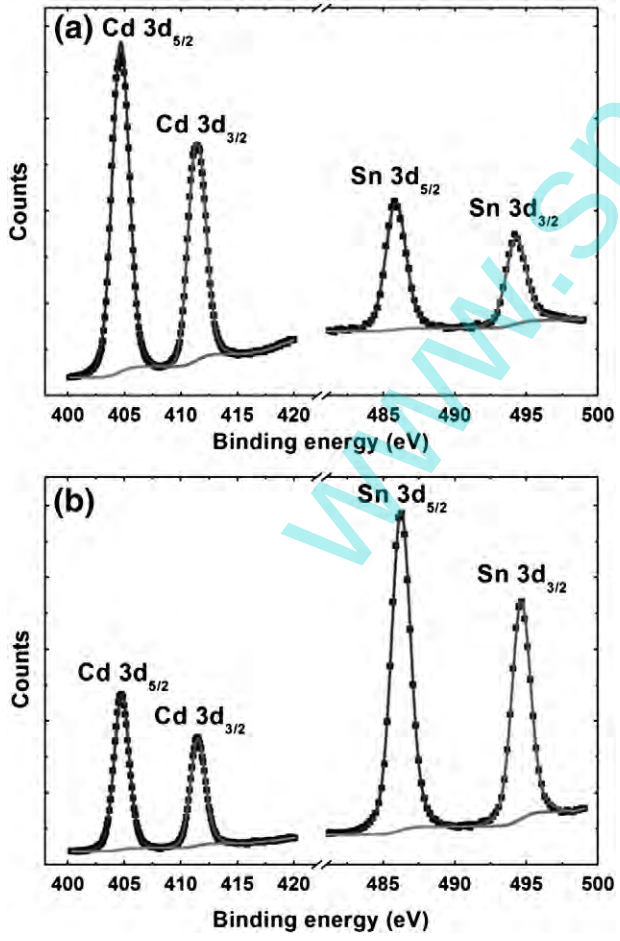

Fig. 2. XPS spectra of the films: (a) $Cd_{0.2}Sn_{0.8}O$ and (b) $Cd_{0.4}Sn_{0.6}O$.

3.3. Electric properties

The electric properties of the $Cd_xSn_{1-x}O$ films were summarized in Table 1. All films were n-type semiconductors and electrons were the free charged carriers. The resistivities of the ternary films could be as low as $10^{-4}\ \Omega \cdot cm$, the concentration of the electron was in the order of 10^{20} cm^{-3}, and the mobility was about 15.5–50 cm^2/V s. Cd provided high concentrations and mobilities of the electrons in the multi-component films. Therefore, the resistivities decreased with the increases of the Cd proportions in the films. The electrical properties of the multi-component films were affected not only by the metallic components, but also by the structures of the films. It is reasonable to believe that the lattice deformation might be serious in the films $Cd_{0.8}Sn_{0.2}O$ and $Cd_{0.2}Sn_{0.8}O$ due to Sn doped CdO and Cd doped SnO_2, and the fact is that the mobilities of electrons in both films were low. In other words, the lattice scattering dominated the mobilities of free electrons. Also, the high mobilities of the free electrons could be seen in the multi-component films with similar Cd:Sn ratios (x = 0.7–0.4), and the even higher mobilities in the films without obvious new phrases, i.e. with amorphous structure. The authors in reference [24] pointed out that the free path of electrons in a semiconductor film was only about 10 nm when the concentration was over $\times 10^{20}$ cm^{-3}, which was comparable to the crystal domain sizes here. Therefore, the free electrons were not only trapped by defects in the amorphous structure, but also scattered by the domain fringes and lattice's deformation of the nano-crystalline. The structures with more amorphous proportion and less domain fringes benefit the mobilities of the free electrons. This conclusion was also proved by many recent studies on amorphous oxide TFT [19,39,40].

In general, the structures of $Cd_xSn_{1-x}O$ films varied from nano-crystal, the mixture nano-crystal and amorphous to amorphous by changing the compositions. The transmittance of the films could be

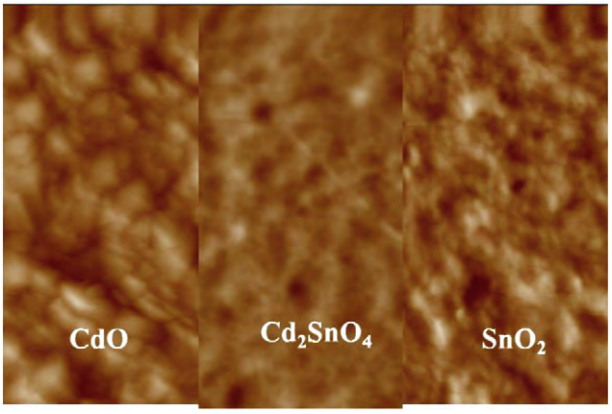

Fig. 3. Typical morphological structures of the $Cd_xSn_{1-x}O$ films by AFM.

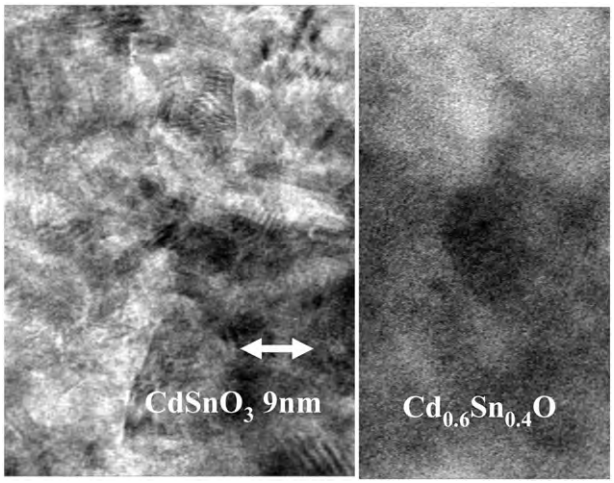

Fig. 4. Typical TEM micro-structures of the $Cd_xSn_{1-x}O$ films.

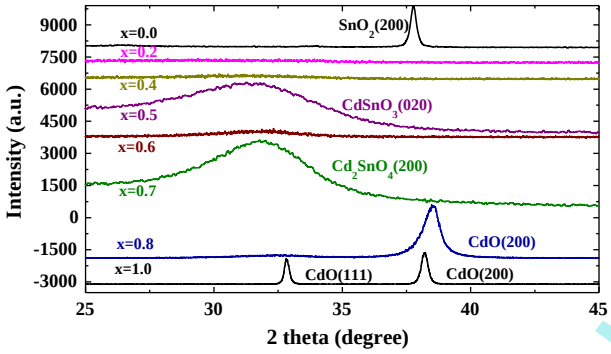

Fig. 5. θ–2θ XRD spectra of the $Cd_xSn_{1-x}O$ films.

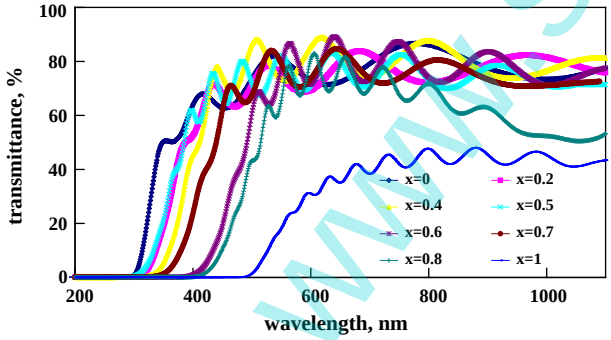

Fig. 6. Transmittance spectra of the $Cd_xSn_{1-x}O$ films deposited on glass slides from blended powder targets.

improved by adding the SnO_2 into CdO, the band gaps enlarged as well. The electron's mobility decreased for the $Cd_xSn_{1-x}O$ ($0<x<1$) films with nano-crystal structure due to the scattering mechanisms by domain fringe and lattice deformation. In another word, high electron's mobility was benefit from the amorphous structure because there was no fringe potential for the electron to overcome. The electron concentrations of the films increased and resistivities decreased with the increases of Cd ratios in the films. By carefully controlling the deposition process, such as the input part of oxygen in argon atmosphere, the low concentration and high mobility of the amorphous $Cd_xSn_{1-x}O$ films may be prepared, which will be carried out in the future research.

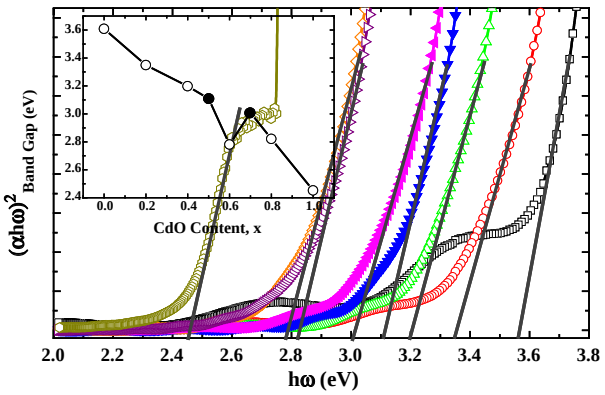

Fig. 7. The $(\alpha h\omega)^2$~hω curves of the $Cd_xSn_{1-x}O$ films converted from transmittance spectra (with band gap figure inside).

4. Conclusions

1. The $Cd_xSn_{1-x}O$ films prepared by RF from powder targets were columnar in over 100 nm grain size. The surfaces of the ternary films were much smoother than those of the pure oxide films.
2. The resistivities of $Cd_xSn_{1-x}O$ films decreased with the increases of Cd proportion and were as low as 10^{-4} Ω·cm, and the concentrations of electrons increased. The mobilities of electrons could be up to 50 cm^2/V s when the Cd:Sn ratio was 3:2.
3. The structures of $Cd_xSn_{1-x}O$ ($x=0.4$–0.7) films were the mixture of amorphous and nano-crystal or amorphous, which benefits the electron mobility.
4. The electron mobilities of the $Cd_xSn_{1-x}O$ films ($x=0.2$ and 0.8) were low due to the scattering by severe lattice deformation and nano-fringe.
5. The transmittance of the ternary $Cd_xSn_{1-x}O$ films was about 80% within the visible wavelength. The band gaps can be adjusted by changing the Cd:Sn ratios.

Acknowledgment

The authors would like to thank professor Xing-Yuan Liu in the Changchun Institute of Optics, Fine Mechanics and Physics, Chinese Academy of Science for his help with the Hall Effect and spectrophotometer measurements. Thanks go to Manger Da-Min Chen, from Yuandong Vacuum Ltd., for the contribution of the rig.

This work is supported by the National Natural Science Foundation of China under the grant Nos. 50872048 and 51172101.

References

[1] E. Fortunato, A. Gonçalves, A. Pimentel, P. Barquinha, G. Gonçalves, L. Pereira, I. Ferreira, R. Martins, Appl. Phys. A 96 (1) (2009) 197.
[2] K. Tonooka, H. Bando, Y. Aiura, Thin Solid Films 445 (2) (2003) 327.
[3] L. Raniero, I. Ferreira, A. Pimentel, A. Gonçalves, P. Canhola, E. Fortunato, R. Martins, Thin Solid Films 511–512 (0) (2006) 295.
[4] S.J.C. Irvine, D.A. Lamb, V. Barrioz, A.J. Clayton, W.S.M. Brooks, S. Rugen-Hankey, G. Kartopu, Thin Solid Films 520 (4) (2011) 1167.
[5] H.-K. Kim, I.-K. You, J.B. Koo, S.-H. Kim, Surface and Coatings Technology (in press) (Available online 24 September 2011).
[6] E. Fortunato, P. Nunes, A. Marques, D. Costa, H. Águas, I. Ferreira, M.E.V. Costa, M.H. Godinho, P.L. Almeida, J.P. Borges, R. Martins, Surf. Coat. Technol. 151–152 (0) (2002) 247.
[7] P.J. Kelly, Y. Zhou, J. Vac. Sci. Technol., A 24 (5) (2006) 1782.
[8] Y. Zhou, P.J. Kelly, Thin Solid Films 469–470 (0) (2004) 18.
[9] J. Robertson, R. Gillen, S.J. Clark, Thin Solid Films 520 (10) (2012) 3714.
[10] H. Yabuta, M. Sano, K. Abe, T. Aiba, T. Den, H. Kumomi, K. Nomura, T. Kamiya, H. Hosono, Appl. Phys. Lett. 89 (11) (2006) 112123.
[11] B. Yaglioglu, H.Y. Yeom, R. Beresford, D.C. Paine, Appl. Phys. Lett. 89 (6) (2006) 062103.
[12] D.H. Yoon, S.J. Kim, W.H. Jeong, D.L. Kim, Y.S. Rim, H.J. Kim, J. Cryst. Growth 326 (1) (2011) 171.
[13] J.S. Park, W.-J. Maeng, H.-S. Kim, J.-S. Park, Thin Solid Films 520 (6) (2012) 1679.

[14] P. Carreras, A. Antony, F. Rojas, J. Bertomeu, Thin Solid Films 520 (4) (2011) 1223.
[15] W.H. Jeong, G.H. Kim, D.L. Kim, H.S. Shin, H.J. Kim, M.-K. Ryu, K.-B. Park, J.-B. Seon, S.-Y. Lee, Thin Solid Films 519 (17) (2011) 5740.
[16] J.C. Moon, F. Aksoy, H. Ju, Z. Liu, B.S. Mun, Curr. Appl. Phys. 11 (3) (2011) 513.
[17] H.C. Ma Damisih, J.-J. Kim, H.Y. Lee, Thin Solid Films 520 (10) (2012) 3741.
[18] S. Lee, H. Park, D.C. Paine, Thin Solid Films 520 (10) (2012) 3769.
[19] K. Ide, Y. Kikuchi, K. Nomura, T. Kamiya, H. Hosono, Thin Solid Films 520 (10) (2012) 3787.
[20] K. Abe, K. Takahashi, A. Sato, H. Kumomi, K. Nomura, T. Kamiya, H. Hosono, Thin Solid Films 520 (10) (2012) 3791.
[21] G. Socol, D. Craciun, I.N. Mihailescu, N. Stefan, C. Besleaga, L. Ion, S. Antohe, K.W. Kim, D. Norton, S.J. Pearton, A.C. Galca, V. Craciun, Thin Solid Films 520 (4) (2011) 1274.
[22] S. Lee, B. Bierig, D.C. Paine, Thin Solid Films 520 (10) (2012) 3764.
[23] D.-H. Kim, W.-J. Kim, S.J. Park, H.W. Choi, K.-H. Kim, Surf. Coat. Technol. 205 (Supplement 1/0) (2010) S324.
[24] T.J. Coutts, D.L. Young, X. Li, W.P. Mulligan, X. Wu, J. Vac. Sci. Technol., A 18 (6) (2000) 2646.
[25] J. Santos-Cruz, G. Torres-Delgado, R. Castanedo-Perez, S. Jiménez-Sandoval, O. Jiménez-Sandoval, C.I. Zúñiga-Romero, J. Márquez Marín, O. Zelaya-Angel, Thin Solid Films 493 (1–2) (2005) 83.
[26] M. Yan, M. Lane, C.R. Kannewurf, R.P.H. Chang, Appl. Phys. Lett. 78 (16) (2001) 2342.
[27] B. Saha, R. Thapa, K.K. Chattopadhyay, Sol. Energy Mater. Sol. Cells 92 (9) (2008) 1077.
[28] A. Fouzri, M.A. Boukadhaba, M. Oumezzine, V. Sallet, Thin Solid Films 520 (7) (2012) 2582.
[29] A.A. Ziabari, F.E. Ghodsi, Thin Solid Films 520 (4) (2011) 1228.
[30] R. Mamazza Jr., D.L. Morel, C.S. Ferekides, Thin Solid Films 484 (1–2) (2005) 26.
[31] H.M. Ali, H.A. Mohamed, M.M. Wakkad, M.F. Hasaneen, Thin Solid Films 515 (5) (2007) 3024.
[32] C.A. Barboza, J.M. Henriques, E.L. Albuquerque, E.W.S. Caetano, V.N. Freire, J.A.P. da Costa, Chem. Phys. Lett. 480 (4–6) (2009) 273.
[33] C.A. Barboza, J.M. Henriques, E.L. Albuquerque, E.W.S. Caetano, V.N. Freire, J.A.P. da Costa, J. Solid State Chem. 183 (2) (2010) 437.
[34] W. Yang, Y.W. Zhou, C.Y. Zheng, F.Y. Wu, J. Liu, In: Electronics and Optoelectronics (ICEOE), IEEE, Dalian, Liaoning, 2011, p. V4.
[35] F.-Y. Wu, Zhou Yan-Wen**, Zheng Chun-Yan, Chin. Phys. Lett. 28 (10) (2011) 107307.
[36] Y. Zhou, P. Kelly, Q.B. Sun, Thin Solid Films 516 (12) (2008) 4030.
[37] Y. Zhou, PhD, University of Salford, Manchester, 2005.
[38] D.Y. Lee, J.R. Lee, G.H. Lee, P.K. Song, Surf. Coat. Technol. 202 (22–23) (2008) 5718.
[39] K. Lee, K. Nomura, H. Yanagi, T. Kamiya, H. Hosono, Thin Solid Films 520 (10) (2012) 3808.
[40] K. Nomura, T. Kamiya, H. Hosono, Thin Solid Films 520 (10) (2012) 3778.